Colloids and Surfaces B: Biointerfaces 206 (2021) 111927

Contents lists available at ScienceDirect

Colloids and Surfaces B: Biointerfaces

journal homepage: www.elsevier.com/locate/colsurfb

Modeling the saturation of detergent association in mixed liposome systems☆

Samantha T. Clark [a], Matthias M.L. Arras [b,1], Stephen A. Sarles [c], Paul D. Frymier [a,*]

[a] Department of Chemical and Biomolecular Engineering, University of Tennessee, Knoxville, 1512 Middle Dr, Knoxville, TN 37996, USA
[b] Neutron Scattering Division, Oak Ridge National Laboratory, Oak Ridge, TN 37831, USA
[c] Department of Mechanical, Aerospace, and Biomedical Engineering, University of Tennessee, 1512 Middle Drive, 414 Dougherty Engineering Building, Knoxville, TN 37996, USA

ARTICLE INFO

Keywords:
Mixed liposomes
Vesicle
Model
Detergent
Solubilization
Saturation

ABSTRACT

Cells tune the lipid types present in their membranes to adjust for thermal and chemical stability, as well as to promote association and dissociation of small molecules and bound proteins. Understanding the influence of lipid type on molecule association would open doors for targeted cell therapies, in particular when molecular association is observed in the presence of competing membranes. For this reason, we modeled and experimentally observed the association of a small molecule with two membrane types present by measuring the association of the detergent Triton X-100 with two types of liposomes, egg phosphatidylcholine (ePC) liposomes and egg phosphatidic acid (ePA) liposomes, at varying ratios. We called this mixed liposomes, as each liposome population was formed from a different lipid type. Absorbance spectrometry was used to observe the stages of detergent association with mixed liposomes and to determine the detergent concentration at which the liposomes were fully saturated. A saturation model was also derived that predicts the detergent associated with each liposome type when the lipid bilayers are fully saturated with detergent. The techinical input parameters for the model are the detergent to lipid ratio and the relative absorbance intensity for each of the pure liposome species at saturation. With that, the association of detergent with any mixture of those liposome types at saturation can be determined.

1. Introduction

One method that nature uses to regulate the association of small molecules with cells and organelles is tuning lipid compositions to encourage and discourage association [1]. This affinity can be studied *in vitro* using synthetic lipid membranes called large unilamellar vesicles (LUVs), referred to in this paper as liposomes. Detergent is an example of a small molecule that has been examined in depth with regards to liposome association [2]. These studies have observed a systematic uptake of detergent by liposomes with increasing detergent concentrations until saturation is achieved. Increasing the detergent concentration further leads to a step-wise dissociation of saturated liposomes into micelles composed of a mixture of lipid and detergent molecules [3–5] (see Supplemtary Fig. S1). The bulk of knowledge on detergent solubilization of liposomes has been acquired on liposomes made with a single lipid. More recently, studies emerged on detergent solubilization of mixed-lipid liposomes, liposomes containing more than one lipid type [6–17]. A new, so far unexplored, horizon is the detergent solubilization of liposomes made from A-type lipids in the presence of liposomes made from B-type lipids. For example, 50% of the liposomes are made from one type of lipids, which may represent one native membrane type, and the other 50% of the liposome are made of a different type of lipids, which represents a second native membrane type. We call the result a mixed liposome (colloidal) dispersion to differentiate it from a

☆ This manuscript has been co-authored by UT-Battelle, LLC under Contract No. DE-AC05-00OR22725 with the U.S. Department of Energy. The United States Government retains and the publisher, by accepting the article for publication, acknowledges that the United States Government retains a non-exclusive, paid-up, irrevocable, worldwide license to publish or reproduce the published form of this manuscript, or allow others to do so, for United States Government purposes. The Department of Energy will provide public access to these results of federally sponsored research in accordance with the DOE Public Access Plan (http://energy.gov/downloads/doe-public-access-plan).

* Corresponding author.
E-mail address: pdf@utk.edu (P.D. Frymier).
[1] Present address: DSM, Materials Science Center, Urmonderbaan 22, 6167RD Geleen, The Netherlands.

https://doi.org/10.1016/j.colsurfb.2021.111927
Received 22 March 2021; Received in revised form 8 June 2021; Accepted 14 June 2021
Available online 17 June 2021

dispersion of mixed-lipid liposomes. Fig. 1 demonstrates these two types of liposome dispersions, where red and blue represent two different lipid types A and B.

Studying the association of a small molecule with mixed liposomes will give insight into the governing principles of this interaction. This has applications for example for targeted drug delivery, where a target molecule shall be guided to a particular organ, enabled by the distinct composition of the organ's membrane. This paper seeks to open that door of research by expanding on a well-known system, detergent association with liposomes. Here we study detergent association with liposomes when there are two populations of liposomes present, each made of different lipid types. To add extra value to this study, we also derive a set of equations that predict the association of the small molecule with each membrane/liposome type present. The model uses only experimental data for the association of small molecules with each of the individual liposome populations, and it predicts the number of detergent molecules bound with each of the liposome types.

To begin, we chose egg phosphatidylcholine (ePC) liposomes and egg phosphatidic acid (ePA) liposomes. These are well characterized lipids that contain a similar distribution of fatty acid chains and have head groups of quite different natures. ePC is a neutral, cylindrical-shaped lipid, while ePA is negatively charged, conical-shaped lipid. The shape of each of these lipids results in quite different detergent association rates [6]. This rendered them great candidates for studying a mixture of two distinct populations of liposomes. In this paper, absorbance and dynamic light scattering have been used to observe the saturation of mixed liposomes with detergent, and a saturation model has been derived that describes the data.

2. Materials and methods

2.1. Materials

Buffers were prepared from potassium phosphate, sodium sulfate, and potassium sulfate, all purchased from Fisher Scientific (Hampton, NH). Aqueous buffer solutions for all experiments contained 25 mM KH_2PO_4-KOH pH 7, 50 mM Na_2SO_4, and 50 mM K_2SO_4. Powder lipids were purchased from Avanti Polar Lipids, Inc. (Alabaster, AL). These included 1,2-dipalmitoyl-sn-glycero-3-phosphochline (16:0PC), 1,2-dipalmitoyl-sn-glycero-3-phosphate (sodium salt) (16:0PA), chicken egg phosphatidylcholine (ePC), and chicken egg phosphatidic acid (ePA). The carbon chain-lengths distribution for ePC and ePA can be found in Table S3. Triton X-100 detergent (<3% polyethylene glycol) and chloroform (99.8% pure) were purchased from Sigma-Aldrich (St. Louis, MO). Detergent and lipids were used without further purification.

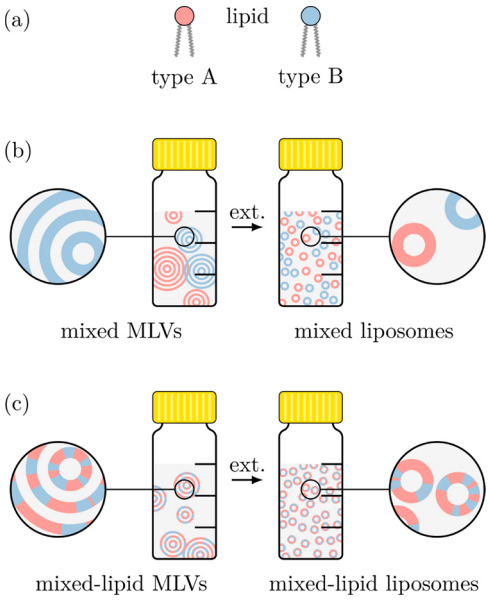

Fig. 1. Depiction of multilamellar vesicles (MLVs) extruded (ext.) into liposomes. Blue and red are used to represent two different types of lipids (a). In (b), MLVs of two different lipid types are mixed together, then extruded to form mixed liposomes, and in (c), mixed-lipid MLVs are extruded to form mixed-lipid liposomes. This paper examines detergent association with mixed liposomes, as in (b) right-hand side.

2.2. Liposome preparation

Fig. 2 depicts the preparation procedure described in this section for forming mixed liposomes. The here described procedure was performed individually for each liposome type (16:0PC, 16:0PA, ePC and ePA) to obtain MLVs of each. To start, MLVs were formed by dissolving purchased powdered lipids with chloroform and aliqoted to a desired lipid unit per vial. The chloroform was removed by vacuum desiccation overnight, forming a thin lipid film on the vial walls. The prepared lipid films were stored at −20 °C. Immediately prior to use, lipid films were hydrated in a potassium phosphate buffer, pH 7.2, containing 25 mM KH_2PO_4-KOH pH 7, 50 mM Na_2SO_4, and 50 mM K_2SO_4. Samples were heated above melting temperature (T_m) and vortexed to thoroughly suspend the lipids and form multilamellar vesicles (MLVs) [18]. ePC and ePA were soluble at room temperature, thus did not need to be heated. After solubilizing the lipids, the MLVs were subjected to four freeze-thaw cycles at −20 °C and 10 °C above the lipid T_m. The mixed liposomes were then made by combining and diluting the individual MLV dispersions, then extruding the dispersion at 10 °C above the highest T_m. 31 repetitive extrusions were performed with an Avanti Mini-Extruder system fitted with a Whatman 100 nm Nuclepore Track-Etch membrane (model 800309) to form liposomes.

In the preparation of mixed liposomes, MLVs of the respective lipid type were mixed together prior to extrusion. For the mixed-lipid MLVs used in calorimetry experiments, the two lipid types solubilized in chloroform were mixed together, then desiccated to form a lipid film comprised of both lipid types. This results in mixed-lipid liposomes. All preparations were used immediately.

2.3. Differential scanning calorimetry

Differential scanning calorimetry (DSC) was used to determine the melting temperature(s) of the lipid bilayers in order to observe the number of distinct vesicle populations in dispersion. DSC samples were prepared as outlined in Section 2.2 using 16:0PC and 16:0PA. The mixed MLVs, mixed-lipid MLVs and mixed liposomes samples were each made with 2 mg/ml 16:0PC and 2 mg/ml 16:0PA. The MLV samples were not extruded. Each lipid sample and deionised water reference were placed under vacuum for 15 min with a stir bar rotating at 600 rpm to degas prior to use. Measurements were made using a TA Instruments NanoDSC calorimeter with 0.5 ml chambers at 0.3 MPa. Samples were equilibrated at 30 °C for 110 min before and in-between each of the 3 heating-cooling cycles, which ran from 30 to 70 °C at scan rates of 1, 0.25, and 0.25 °C/min. The third heating run was analyzed.

2.4. Absorbance spectrophotometry

The detergent saturation and solubilization concentrations of prepared liposome dispersions were determined using absorbance spectrophotometry. This technique indirectly observes the size dependent change in absorbance, which occurs due to detergent interactions with liposomes. For these measurements, liposomes were prepared by extrusion, then allowed to equilibrate for 30 min at room temperature. The prepared liposomes were added to vials containing TX dilutions from 0 to 20 mM and equilibrated at room temperature for 30 min. It should be noted that in all dispersions with TX present, the TX concentration was at least one order of magnitude above its critical micelle

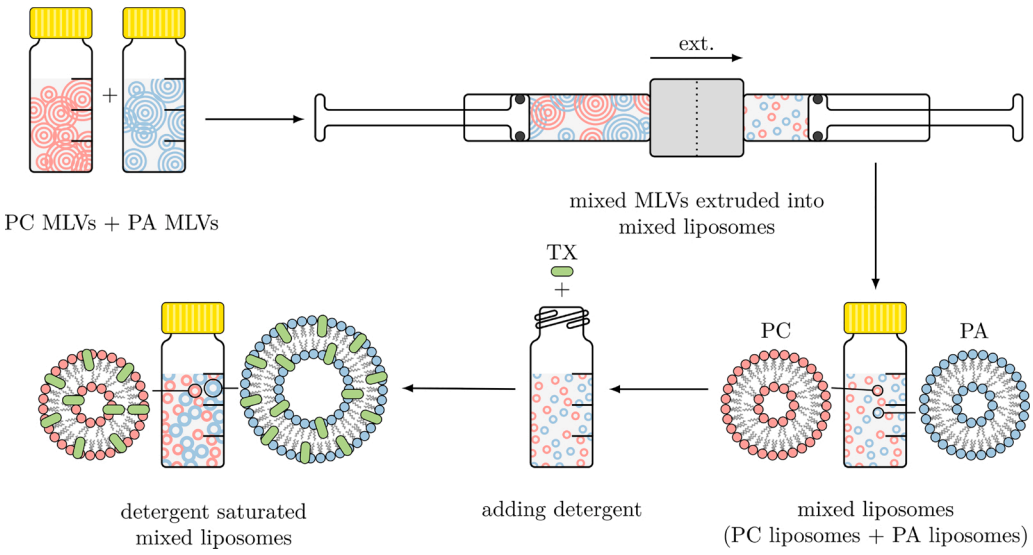

Fig. 2. Depiction of the preparation procedure to form mixed liposomes. Starting at the top-left, PC and PA are hydrated in separate vials to form PC MLVs and PA MLVs. The PC MLVs and PA MLVs are mixed, then loaded into a syringe (top-right). The MLVs are extruded through a 100 nm pore-membrane to form a mixture of PC liposomes and PA liposomes, called mixed liposomes (bottom-right). TX detergent is added to the mixed liposomes (bottom-center), which may yield detergent saturated mixed liposomes (bottom-left).

concentration (0.22–0.24 mM [19]). After the TX and liposome dispersions equilibrated, absorbance measurements were taken using the pedestal reader of a Thermo-Scientific NanoDrop 2000c spectrophotometer. Turbidity data was recorded at 400 nm and a full UV-Vis sweep was used to ensure that there were no air pockets or irregularities in the samples. For each mixed liposome composition, three preparations were made and each sample was tested in triplicate on the spectrophotometer (resulting in 9 measurements per data point). The absorbance readings at 400 nm were normalized to 1 for the pure liposome dispersions, of which, an average and standard deviation from these normalized curves are reported. D_{sat} and D_{sol} were determined from the TX concentration dependent absorbance curves using the detergent concentration at the peak absorbance and the detergent concentration beyond which absorbance no longer changes significantly with increasing detergent concentrations [6].

2.5. Dynamic light scattering

To complement turbidity measurements, dynamic light scattering (DLS) was performed to determine the particle size and distribution at concentrations of interest, including post-extrusion lipid-only liposomes with no TX and fully solubilized liposomes. DLS samples were prepared in the same manner as for absorbance spectrophotometry. Measurements were taken on a DynaPro NanoStar fixed angle dynamic light scattering instrument with 20 × 10 second acquisitions at 20 °C. Three sample sets with duplicates were observed for each lipid-detergent composition. The data were fit to a standard isotropic sphere model at optimal resolution. It is displayed as an average at each TX concentration and lipid composition.

3. Experimental results and discussion

The lipids ePC and ePA have been chosen for two reasons. First, ePC and ePA headgroups are ubiquitous in natural systems. Second, the distribution of chain-lengths in the egg-derived lipids makes this study relevant for naturally occurring membranes.

To begin, experimental evidence is presented that relevant samples considered in this study are indeed a system of mixed ePC liposomes and ePA liposomes. Next, D_{sat} is discussed as a function of the ratio of ePC liposomes to ePA liposomes (ePC:ePA). A schematic depiction of mixed liposomes can be seen in Fig. 1(b), right-hand side. It was observed that D_{sat} as a function of the ratio ePC:ePA does not follow the linear rule of mixtures. This became our initial reason for devising the rate constant model to predict D_{sat} as a function of ePC:ePA that is derived in Section 4.

3.1. DSC evidence for mixed liposomes

Differential scanning calorimetry (DSC) was performed to verify that mixed liposomes were obtained following the protocol outlined in Section 2.2. Specifically, the extent of inter-liposome lipid exchange during extrusion was an open question. Measuring the phase transition temperature (T_m) of membranes from the liquid crystalline state to the gel state provides information on lipid stability and lipid-lipid interactions.

Since T_m of ePC and ePA are known to be below the freezing point of water (0 °C), 16:0PC and 16:0PA, with a known transition above 0 °C, were chosen as surrogates to allow measurements in water. 16:0PC and 16:0PA have the same head group as ePC and ePA, and represent their most prevalent fatty acid chain. For fatty acid chain distribution of ePC and ePA, see Supplementary Section S2.

Fig. 3(a) shows the third DSC heating run for PC MLVs (—) and PA MLVs (—). In DSC, ordered systems that melt show an enthalpic peak at the T_m. For the DSC analysis of membranes it is standard procedure to measure MLVs as they improve the resolution of the measurement [18]. Here, MLVs are analyzed to forecast the number of different membrane compositions present after extruding them into liposomes. The predominant T_m of 16:0PC MLVs is at 42 °C and that of 16:0PA is at 64 °C (see Fig. 3(a)). These narrow peaks are distinctly separated by 22 °C. Additionally, 16:0PC has a pre-transition at 35 °C. These values are substantiated by literature values [18]. In addition, Fig. 3(a) shows the DSC data for a mixture of equal parts 16:0PC MLVs and 16:0PA MLVs (—), labeled mixed MLVs and illustrated by the scheme as established in Fig. 1(b) left-hand side. The mixed MLVs sample shows two T_m values at nearly the same positions (42 and 64 °C) as for the individual MLV dispersions, but with lower molar heat capacity. This indicates there were two different membrane compositions present with little to no exchange of lipids between the populations when combined in a vial.

As previously indicated, it is commonly accepted that extrusion of MLVs into liposomes broadens the observed peaks in DSC [18]. Fig. 3(b) shows that as a result of extrusion, melting peaks for mixed liposomes (—) were broadened in comparision to the unextruded mixed MLVs (—). In brief, this broadening of the melting peak may be explained by the lower number of lipids available for coordination in a single lipid bilayer. In multilamellar systems, there is an extended long-range order that disintegrates simultaneously at the melting point releasing energy all at once, resulting in a sharper peak [18]. Some of the broadening may also be due to exchange of lipid molecules between the different lipid liposomes. Lipid exchange, however, is likely of secondary importance, because predominant lipid exchange would also broaden the peaks for mixed MLVs, which was not observed. Despite the broadening, mixed

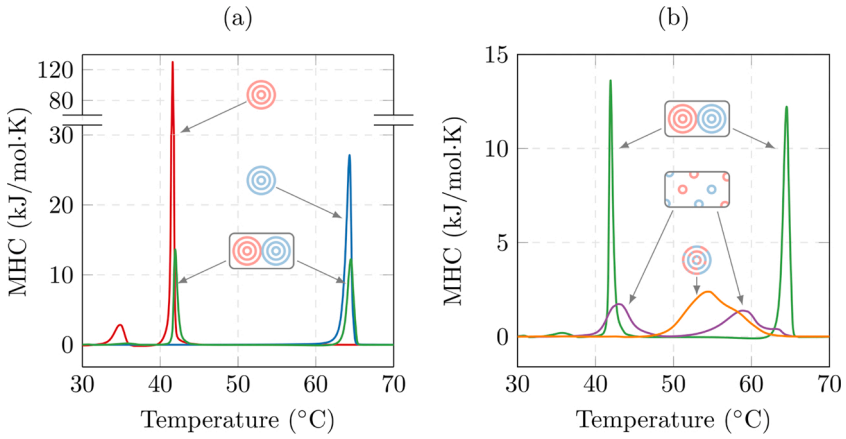

Fig. 3. Results of DSC measurements for various vesicles: (a) PC MLVs (—), PA MLVs (—), and mixed MLVs (—); (b) mixed liposomes (—), mixed-lipid MLVs (—), and mixed MLVs (—). This shows that samples of mixed liposomes contain two distinct species of liposomes, whereas mixed-lipid MLVs are clearly one membrane species.

liposomes show two distinct melting transitions for each lipid and the peaks are still clearly separated. This indicates that there are two distinct liposome populations with very little lipid mixing between the different membranes.

As a control, the transition temperature of mixed-lipid MLVs (—) was observed to demonstrate that bilayers containing both lipids shows only one peak in DSC (see Fig. 3(b)). Indeed for this sample, a singular broad transition region at 54 °C was found. Thus, this method produced a population of liposomes with both lipids mixed together in the bilayers, whereas the before-mentioned mixed liposomes extrusion method produced two distinct liposome populations. An alternative method for preparing mixed liposomes could be to extrude lipid types separately, then mix them together. The DSC data presented here shows for the first time that applying the simpler, single extrusion method on two MLV populations produces liposomes with two distinct membrane compositions.

In all later sections, liposome preparations follow the protocol for preparing mixed liposomes, i.e., pre-hydrated lipid MLVs are mixed, then extruded together to form two distinct liposome populations.

3.2. Spectrophotometry characterizes association of TX with mixed liposomes

The association of TX with mixed liposomes was observed using absorbance spectrophotometry at 400 nm [3]. As TX associates with liposomes, the liposomes change in size. All other things being equal, larger particles scatter more light than smaller particles, causing an increase in observed absorbance. A schematic depiction exemplifying the changes of liposome size as TX concentration is increased is shown in Fig. S1. The schematic shows that TX molecules partition and incorporate into liposomes, causing an increase in liposome diameter. Under further TX addition, the liposomes continue to swell until a TX concentration is reached in which liposomes are saturated with detergent. This point is defined as the D_{sat} concentration. Upon further increase in TX concentration, liposomes reduce in size as mixed-micelles, comprised of lipid and detergent molecules, bud off of the liposomes. Liposomes are fully solubilized once all liposomes have been converted into mixed-micelles. The concentration of TX when this initially occurs is D_{sol}. This is observed by the onset of a base-line in absorbance.

In this study, mixed liposome dispersions were prepared from ePC and ePA liposomes at mass ratios of 100:0, 75:25, 50:50, 25:75, and 0:100 ePC:ePA. DSC results presented in Section 3.1 show that PC liposomes and PA liposomes are both present without lipid exchange between the two liposome populations. The average extruded diameter of liposomes in the mixed liposome dispersions did not change with composition. On average, the diameter was 123 ± 3 nm, as measured by DLS and shown in Table 1 and Fig. S2.

Fig. 4 shows the absorbance spectrophotometry results as a function of TX concentration for each mixed liposome ratio. The absorbance curves follow the expected trend shown in Fig. S1. Generally speaking, curves are shifted up and to the right with increasing ePA liposome concentration. Of all samples, pure ePC liposomes (100:0 ePC:ePA, ●) exhibited the lowest peak absorbance and the lowest TX concentration (1.1 mM TX) at D_{sat}, along with the lowest D_{sol} concentration (7 mM TX). In contrast, pure ePA liposomes (0:100 ePC:ePA, ●) exhibited the highest peak absorbance and the highest TX concentration (2.6 mM TX) at D_{sat}, along with the highest D_{sol} concentration (12.15 mM TX). Additionally, the stage between D_{sat} and D_{sol}, in which saturated liposomes and mixed-micelles are present, spanned a wider range of TX concentrations for pure ePA liposomes than for pure ePC liposomes (9.6–6.9 mM). This is consistent with pure ePA liposomes reaching D_{sat} at a much higher TX concentration than pure ePC liposomes. The absorbance curves in Fig. 4 for mixed liposome dispersions (75:25, ●; 50:50, ; 25:75, ●) lie between the curves of the pure liposomes. The D_{sat} concentrations derived from these curves are plotted in Fig. 4 inset. Evidently, in mixed ePC liposome and ePA liposome dispersions, D_{sat} increases with an increasing percentage of ePA liposomes.

In Fig. 4 inset, the weighted mean rule of mixtures was applied to the pure liposome data (D_{sat} at 100:0 is D^A_{sat}, and D_{sat} at 0:100 is D^B_{sat}) to predict D_{sat} of mixed liposomes as a function of composition. The general equation for D_{sat} of mixed liposomes as the weighted mean is $D_{sat}(x_b) = x_a D^A_{sat} + x_b D^B_{sat}$ where $x_a + x_b = 1$. Here, x_a and x_b are the mole fractions of A-type and B-type lipids.

Table 1
The average diameter of particles measured by DLS as a function of mixed liposome composition, ePC:ePA. This confirms a similar starting size of prepared liposomes for all lipid compositions and similar mixed-micelle size above TX concentrations needed for full solubilization of liposomes.

ePC:ePA	Diameter (nm) TX concentration (mM)	
	0.0[a]	>15[b]
100:0	126.1 ± 2.8	19.9 ± 3.4
75:25	125.4 ± 1.5	18.1 ± 3.3
50:50	118.4 ± 4.7	19.7 ± 0.7
25:75	123.0 ± 2.7	19.4 ± 1.4
0:100	121.7 ± 3.5	17.8 ± 2.3

[a] Liposomes.
[b] Liposomes fully solubilized into mixed-micelles.

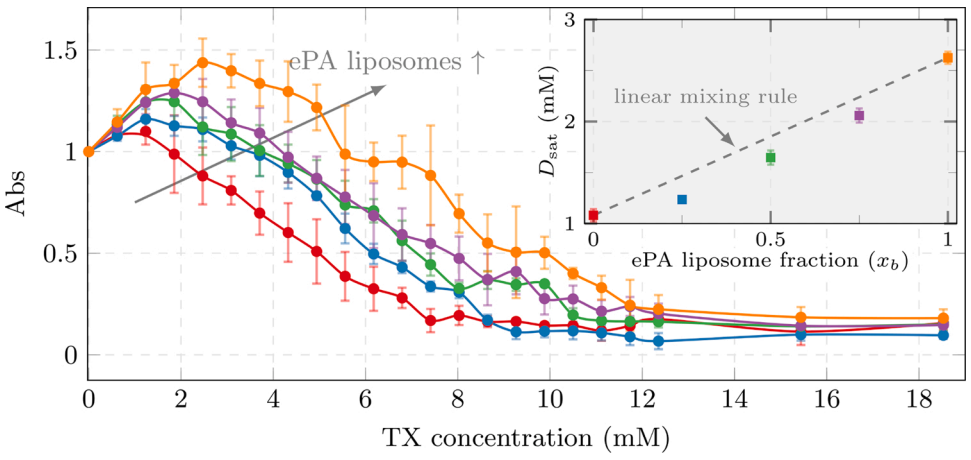

Fig. 4. Normalized absorbance (Abs) of mixed ePC liposomes:ePA liposomes dispersions at ratios of 100:0 (●), 75:25 (●), 50:50 (●), 25:75 (●), and 0:100 (●) under increasing TX concentration. Lines are a guide to the eye. Generally speaking, curves are shifted up and to the right with increasing ePA liposome concentration. Inset: The concentration of TX at saturation, D_{sat}, was determined at the maximum absorbance for the various ePC:ePA ratios (colors corresponding) displayed as a function of molar ePA liposome fraction (x_b). To understand the relationship between mixed liposome composition and D_{sat}, the linear mixing rule was fit to the pure liposome data (– – –). The linear mixing rule over-predicts experimental data for the mixed liposome ratios 25:75, 50:50, and 75:25. An improved model, able to predict these values is presented in Section 4.

For mixed ePC and ePA liposomes, the weighted mean curve over-predicts D_{sat}, meaning that the TX concentrations required to saturate the mixed liposomes are lower in reality than predicted (see Fig. 4 inset). A coefficient of determination (R^2) value for this fit is 0.62. This R^2 was calculated between experimental data and the predictive model at 25:75, 50:50, and 75:25 ePC:ePA. To find a better prediction of D_{sat} for mixtures of liposomes, a saturation model was derived and applied in Section 4.

4. Saturation model

As seen above, a simple weighted mean (linear) interpolation of D_{sat} values of pure liposome data is not a good predictor of D_{sat} for mixed liposomes (see Fig. 4 inset). A mechanistic model for mixed liposomes was derived to improve the prediction. The derivation follows the superposition principle, i.e., mixing A-type and B-type liposomes together does not change the governing characteristics of the individual species. One prerequisite is that lipid exchange between liposome species is negligible, which is in line with experimental results for the considered system (see Section 3.1). In addition to predicting D_{sat}, this model estimates the number of detergent molecules associated with each liposome species at saturation if all other conditions are kept constant, i.e., temperature, pH, etc.

The derivation begins with an equilibrium expression for the association of detergent with A-type liposomes:

$$[A] + [D_W] \overset{K_A}{\rightleftharpoons} [D_A] \tag{1}$$

and an equilibrium expression for the association of detergent with B-type liposomes:

$$[B] + [D_W] \overset{K_B}{\rightleftharpoons} [D_B]. \tag{2}$$

Here, $[A]$ and $[B]$ are the total concentrations of ePC and ePA lipids in dispersion, respectively. $[D_W]$ is the concentration of detergent in solution not associated with a liposome, which can either be freely solubilized or aggregated in micelles. The concentrations of detergent (here TX) associated with either A-type or B-type liposomes are then called $[D_A]$ or $[D_B]$, respectively. The equilibrium constants for K_A and K_B are therefore:

$$K_A = \frac{[D_A]}{[A][D_W]} \tag{3}$$

and

$$K_B = \frac{[D_B]}{[B][D_W]}. \tag{4}$$

As liposomes approach saturation, the total concentration of detergent added ($[D_T]$), must be either in solution or incorporated into A-type or B-type liposomes. Therefore, the mass balance for total detergent is:

$$[D_T] = [D_W] + [D_A] + [D_B]. \tag{5}$$

The equilibrium constants K_A and K_B are calculated from pure liposome data at saturation. Assuming A-type liposomes and B-type liposomes do not exchange lipids significantly, and the presence of A-type liposomes does not affect the fraction of sites available for detergent adsorption in B-type liposomes (and vice-versa), then the rate constants can be expressed in terms of the maximum fraction of detergent sites per lipid in A-type liposomes, n, as:

$$K_A = \frac{n}{[D^*_{T_{A_0}}] - n[A_0]} \tag{6}$$

and the maximum fraction of detergent sites per lipid in B-type liposomes, m, as:

$$K_B = \frac{m}{[D^*_{T_{B_0}}] - m[B_0]}. \tag{7}$$

In these expressions, an asterisk (*) is used to denote saturation conditions. $[D^*_{T_{A_0}}]$ and $[D^*_{T_{B_0}}]$ are the total detergent concentrations at saturation for pure A-type liposomes at concentration $[A_0]$ and pure B-type liposomes at concentration $[B_0]$, respectively.

One can determine the number of detergent molecules associated with each liposome type, n or m, if the following parameters are known: change in liposome size due to association, the area per detergent molecule in the liposomal bilayer (σ), and the number of liposomes (N_A) (see page s5 and following for details):

$$n[A_0] = N_A \frac{8\pi}{\sigma} \left({r^*_{A_0}}^2 - {r^0_{A_0}}^2 \right) \tag{8}$$

Herein, the assumption was made that the liposomal bilayer thickness is small in comparison the radius of pristine pure A-type liposomes ($r^0_{A_0}$). $r^*_{A_0}$ is the liposome radius at saturation for pure A-type liposomes. A similar equation holds for B-type liposomes, which then allows m to be expressed in terms of n. In the present publication and the majority of literature in the field, absorbance is used to determine D_{Sat}, instead of directly measuring liposome radius. Therefore, to relate absorbance data to liposome radius (r), a published relationship between these two parameters was used (see Fig. 5 and [20]). Matsuzaki et al. [20] provided

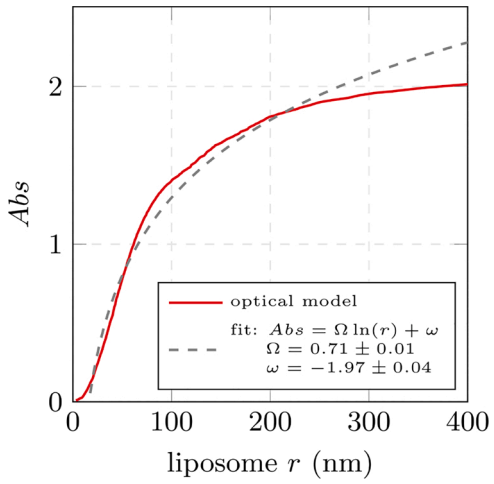

Fig. 5. Simulated optical properties for liposomes at 436 nm by the homogeneous sphere model according to Matsuzaki et al. [20]. Specific optical density as reported in the original publication is transferred to relative *Abs* values by normalizing the curve to unity at 61.5 ± 1.5 nm, which is the average radius of pure ePC or ePA liposomes (diameter is 123 ± 3 nm; compare with Table 1 and Fig. 4).

an example dataset for an absorbance wavelength of 436 nm, which is reasonably close to the 400 nm wavelength used in this publication. The optical model of Matsuzaki et al. [20] can be used to predict the relationship for any applicable wavelength. Within the relevant range of $r = [0,250]$ nm, this relationship can be well approximated by a logarithmic function (see Fig. 5). Therefore, $m = n\frac{\delta_B}{\delta_A}\frac{\Gamma(\mathrm{Abs}^*_{B_0})-\Gamma(\mathrm{Abs}^0_{B_0})}{\Gamma(\mathrm{Abs}^*_{A_0})-\Gamma(\mathrm{Abs}^0_{A_0})}$, whereby $\Gamma(x) = exp((2(x-\omega))/\Omega)$. Herein, Ω and ω are constant parameters applicable for all liposomes irrespective of type or degree of association as long as the radii are within the relevant range, in which $\Omega = 0.71 \pm 0.01$ and $\omega = -1.97 \pm 0.04$. $\delta_A = 0.64\,\mathrm{nm}^2$ and $\delta_B = 0.52\,\mathrm{nm}^2$ are the reported head-group sizes of ePC and ePA [9].

If the optical model in Fig. 5 was unknown, then a linear interpolation could be used to determine m in terms of n, see Eq. (19) in the supplementary section. This would be less accurate and only appropriate if the change in radius induced by detergent association was small. In principle, any technique that observes a change in the physical size of liposomes with detergent association can be used with this method provided appropriate modifications to the equations. Based on the assumption introduced previously that the two lipids only interact with the detergent and not with each other, a final expression for the total amount of detergent at saturation in a mixture of two types of liposomes can be stated as:

$$D_{\mathrm{sat}} = [D_T^*] = ((1-x_b)n[A_0] + x_b m[B_0]) \times \left(\left(\frac{1-x_b}{\frac{[D^*_{T_{A_0}}]}{n[A_0]} - 1} + \frac{x_b}{\frac{[D^*_{T_{B_0}}]}{m[B_0]} - 1} \right)^{-1} + 1 \right) \quad (9)$$

Again, m can be expressed in terms of n to obtain $[D_T^*](x_b, n)$. x_a and x_b are the mole fractions of lipid A and lipid B in the mixed liposome sample whereby the overall lipid concentration is kept constant ($x_a + x_b = 1$). Eq. (9) is numerically solved to find the solution for n that yields the best fit to the experimental data. The step-by-step derivation of Eq. (9) can be found in Supplementary Section S4. See citation [21] in Supplementary for assumptions related to the bilayer thickness and liposome radius.

5. Saturation model results and discussion

Eq. (9) is a saturation model for predicting the concentration of detergent at saturation of mixed liposomes. In this section, the model is discussed while applying it to the experimental data in Section 3.2. To this end, the model is initialized with the parameters given in Table S4, which are derived from the experimental data sets of pure ePC liposomes and pure ePA liposomes. The parameter of the model, n, was not known a priori, thus the value of n was allowed to vary to determine the best fit to the data. The fit was optimized by calculating the coefficient of determination (R^2) for the differences between the experimental data (at 25:75, 50:50, and 75:25 ePC:ePA) and the model as n varied.

In Fig. 6(a), the optimum solution for the model is displayed (——), where $n = 0.081 \pm 0.003$. For this solution $K_A = 0.11 \pm 0.01\,\mathrm{mol}^{-1}$, $K_B = 1.73 \pm 0.58\,\mathrm{mol}^{-1}$, and $m = 0.495 \pm 0.017$. The error estimation is based on the maximum possible error of n given the measurement uncertainty of the experimental data. For the experimental data set presented here, $m > n$ is plausible because of the following arguments. Liposomes of both types (A and B) start at a size of 123 ± 3 nm (see Table 1) and at all detergent concentration points prior to saturation, pure B-type liposomes have a higher absorbance than pure A-type (ePC) liposomes (see Fig. 4). This means B-type (ePA) liposomes are always bigger than A-type liposomes in this experiment, thus B-type liposomes must associate with more detergent (TX), as liposome size is only a function of detergent association here.

The model solution in Fig. 6(b) shows the interesting behavior that, due to the initial rapid reduction in $[D_W^*]$, (the dotted curve, ·····), Dsat decreases for increasing x_b at small x_b. In more detail, Fig. 6(b) shows the contributions of the water-borne TX that is not associated with liposomes and the associated portion of TX. Both together give the predicted D_{sat} curve. It can be seen that the component of associated TX increases proportionally with increasing x_b. The portion of water-borne TX decreases with increasing x_b. This makes sense as TX has a higher affinity to B-type liposomes as indicated by the result $m > n$.

Using the fitting result together with the equations presented in Section 4, the percentage of detergent incorporated into each liposome population (i.e. $n/(n+1)$ for A-type) can be found. Thus, at saturation, A-type liposomes consist of 7.5 ± 0.3% detergent and 92.5 ± 0.3% A-type lipids and B-type liposomes consist of 33.1 ± 0.8% detergent and 66.9 ± 0.8% B-type lipids. To our knowledge, this is the first time that the maximum fraction of detergent per lipid in mixed liposome samples can be revealed from a simple method like absorbance spectrophotometry. A noteworthy feature of the Dsat curve for the optimal n solution is that for low ePA liposome fractions ($x_b < 0.05$), D_{sat} decreases with increasing x_b. Although R^2 for this solution is high (0.98), it partially lies outside of the area spanned by the linear and inverse mixing rules. As explained above this is due to the rapid reduction in water-borne detergent (see Fig. 6(b)). Additional experimental data for $x_b < 0.25$ would give insight into the physicality of this solution. However, considering the measurement accuracy of absorbance spectrophotometry, it may be challenging to obtain meaningful intermediate values. A more precise technique, such as confocal microscopy or neutron scattering, may overcome this.

A sensitivity analysis of the predicted D_{sat} as a function of n is presented in Fig. S3. It shows that the predicted $D_{\mathrm{sat}}(x_b)$ is quite sensitive to variation in n. For example, at $n = 0.65$, a curve is predicted that follows the linear mixing rule and is clearly not in line with the experimental values. For $n = 0.075$, a curve is predicted that lies within the inverse and linear mixing rule, yet is still reasonably close to the experimental data points.

6. Conclusions

In this paper, TX detergent association with a mixed population of ePC liposomes and ePA liposomes was measured using absorbance

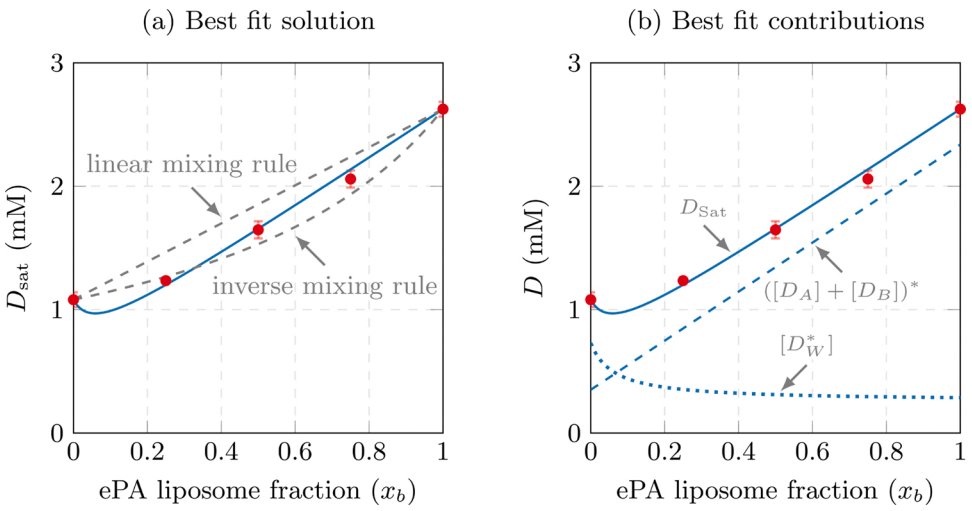

Fig. 6. (a) Optimal solution for the saturation model applied to experimental data presented in Section 3.2 (——). In addition to the linear mixing rule ($R^2 = 0.62$), the inverse mixing rule ($R^2 = 0.91$) is also shown. The saturation model provides the best fit and yields physical information about the system, e.g., the percentage of detergent associated with each liposome type. (b) Contributions of waterborne ($[D_W]$) and associated TX ($[D_A]+[D_B]$) to the total detergent concentration $[D_T]$ for the best fit solution of D_{sat} (see (a)). Detergent in water ($[D_W^*]$, ·····), detergent bound to A-type and B-type liposomes ($([D_A]+[D_B])^*$, - - -), and total detergent in solution (D_{sat}, ——); each at saturation ($D_T^* = D_{sat} = ([D_A]+[D_B])^* + [D_W^*]$).

spectrophotometry. Next, a saturation model was derived that fits experimental data based on an association constant and the geometry of the liposomes. The fundamental assumption of the model is that saturation of each liposome populations is independent of the other, thus the effect of each population on the other is merely to reduce the concentration of unassociated detergent molecules available. Under this assumption, the model can determine the number of detergent sites at saturation for each population (n, m) when the relative lipid headgroup area, δ_A/δ_B, is known. $n = 0.081 \pm 0.003$ and $m = 0.495 \pm 0.017$ were determined using the method of least squares by fitting the model to experimental data to find D_{sat}. These numbers mean that at saturation, ePC can associate with only $7.5 \pm 0.3\%$ TX, whereas ePA can associate with a much higher percentage of TX, $33.1 \pm 0.8\%$. Furthermore, the presented model can be applied to any combination of liposome pairs. After n and m are calibrated with a small data set or independently measured for a liposome pair of interest, all that is needed is information on the detergent saturation of the individual pure liposome populations at the same lipid concentration to fully predict D_{sat} at any combination of liposome mixtures. Saturation data for pure liposomes is readily available in literature or easily accessible through experimentation. Additionally, this saturation model can be expanded to include three or more liposomal species by expanding on the association kinetics.

Abbreviations

$[A]$molar concentration of A-type lipids$[B]$molar concentration of B-type lipids$[D_W]$molar concentration of solubilized detergent in water phase$[D_A]$molar concentration of detergent incorporated with A-type lipids$[D_B]$molar concentration of detergent incorporated with B-type lipids$[D_T]$total molar concentration of detergent$[D^*]$molar concentration of solubilized detergent at saturation$[D_A^*]$molar concentration of detergent incorporated with A-type lipids at saturation$[D_B^*]$molar concentration of detergent incorporated with B-type lipids at saturation$[D_T^*]$total molar concentration of detergent at saturation$[D_{T_{A_0}}^*]$total molar detergent concentration for pure A-type liposomes at saturation$[D_{T_{B_0}}^*]$total molar detergent concentration for pure B-type liposomes at saturation$[A_0]$molar concentration of pure A-type lipids$[B_0]$molar concentration of pure B-type lipids$[D_{A_0}^*]$molar concentration of detergent incorporated with pure A-type lipids at saturation$[D_{B_0}^*]$molar concentration of detergent incorporated with pure B-type lipids at saturation$K_A$association constant for detergent with A-type lipids$K_B$association constant for detergent with B-type lipids$\mathrm{Abs}_{A_0}^*$normalized absorbance for pure A-type liposomes at saturation$\mathrm{Abs}_{B_0}^*$normalized absorbance for pure B-type liposomes at saturation$\mathrm{Abs}_{A_0}^0$normalized absorbance of pristine pure A-type liposomes$\mathrm{Abs}_{B_0}^0$normalized absorbance of pristine pure B-type liposomes$n$fraction of detergent per lipid in A-type liposomes$m$fraction of detergent per lipid in B-type liposomes$x_a$mole fraction of lipid A$x_b$mole fraction of lipid B$h_A$bilayer thickness of A-type liposomes$h_B$bilayer thickness of B-type liposomesΩfitting parameter to convert Abs to $r\omega$fitting parameter to convert Abs to $r\delta_A$headgroup area A-type lipid, here ePC$\delta_B$headgroup area B-type lipid, here ePA$r$average liposome radius$r_{A_0}^0$average radius of pristine pure A-type liposomes$r_{A_0}^*$average radius of saturated pure A-type liposomesσcross-sectional area per detergent molecule in the liposomal bilayer$N_A$number of liposomes in dispersionR^2coefficient of determination DLSdynamic light scatteringDSCdifferential scanning calorimetry$T_m$phase transition temperatureD_{sat}detergent concentration at saturationD_{sol}detergent concentration at solubilizationePAchicken egg-derived PAePCchicken egg-derived PCPAphosphatidic acidPCphosphatidylcholineMHCmeasured heat capacityMLVmulti-lamellar vesiclesTXTriton X-100

Author contributions

Samantha Clark: Conceptualization, methodology, formal analysis, visualization, investigation, writing – original draft, writing – review & editing. Matthias Arras: Formal analysis, visualization, writing – review & editing. Stephen Sarles: Writing – review & editing. Paul Frymier: Conceptualization, resources, writing – review & editing.

Funding

This research was funded through the GAANN Program of the US Department of Education, Award Number P200A120191.

Declaration of Competing Interest

The authors report no declarations of competing interest.

Acknowledgements

We thank Dr. Graham J. Taylor at Oak Ridge National Lab for his consultation and assistance in performing differential scanning calorimetry.

Appendix A. Supplementary data

Supplementary data associated with this article can be found, in the online version, at https://doi.org/10.1016/j.colsurfb.2021.111927.

References

[1] W. Dowhan, M.V. Bogdanov, E. Mileykovskaya, Functional roles of lipids in membranes, in: N.D. Ridgway, R.S. McLeod (Eds.), Biochemistry of Lipids, Lipoproteins and Membranes, 6th ed., Elsevier, 2015, pp. 1–40, https://doi.org/10.1016/B978-0-444-63438-2.00001-8.

[2] D. Lichtenberg, H. Ahyayauch, A. Alonso, F.M. Goñi, Detergent solubilization of lipid bilayers: a balance of driving forces, Trends Biochem. Sci. 38 (2013) 85–93, https://doi.org/10.1016/j.tibs.2012.11.005.

[3] D. Lichtenberg, R.J. Robson, E.A. Dennis, Solubilization of phospholipids by detergents structural and kinetic aspects, BBA – Rev. Biomembr. 737 (1983) 285–304, https://doi.org/10.1016/0304-4157(83)90004-7.

[4] J.R. Silvius, Solubilization and functional reconstitution of bioemembrane components, Annu. Rev. Biophys. Biomol. Struct. 21 (1992) 323–348, https://doi.org/10.1146/annurev.bb.21.060192.001543.

[5] J.L. Rigaud, B. Pitard, D. Levy, Reconstitution of membrane proteins into liposomes: application to energy-transducing membrane proteins, BBA – Bioenergetics 1231 (1995) 223–246, https://doi.org/10.1016/0005-2728(95)00091-V.

[6] S.T. Clark, M.M.L. Arras, S.A. Sarles, P.D. Frymier, Lipid shape determination of detergent solubilization in mixed-lipid liposomes, Colloids Surf. B: Biointerfaces (2019) 110609.

[7] A. De la Maza, J.L. Parra, Vesicle-micelle structural transition of phosphatidylcholine bilayers and Triton X-100, Biochem. J. 303 (1994) 907–914, https://doi.org/10.1042/bj3030907.

[8] H. Ahyayauch, M.I. Collado, A. Alonso, F.M. Goñi, Lipid bilayers in the gel phase become saturated by Triton X-100 at lower surfactant concentrations than those in the fluid phase, Biophys. J. 102 (2012) 2510–2516, https://doi.org/10.1016/j.bpj.2012.04.041.

[9] A. Dickey, R. Faller, Examining the contributions of lipid shape and headgroup charge on bilayer behavior, Biophys. J. 95 (2008) 2636–2646, https://doi.org/10.1529/biophysj.107.128074.

[10] H. Ahyayauch, B. Larijani, A. Alonso, F.M. Goñi, Detergent solubilization of phosphatidylcholine bilayers in the fluid state: Influence of the acyl chain structure, BBA – Biomembranes 1758 (2006) 190–196, https://doi.org/10.1016/j.bbamem.2006.01.016.

[11] M.A. Partearroyo, A. Alonso, F.M. Goñi, M. Tribout, S. Paredes, Solubilization of phospholipid bilayers by surfactants belonging to the Triton X series: effect of polar group size, J. Colloid Interface Sci. 178 (1996) 156–159, https://doi.org/10.1006/jcis.1996.0103.

[12] T.M. Bayer, G.D. Werner, E. Sackmann, Solubilization of DMPC and DPPC vesicles by detergents below their critical micellization concentration, Biochim. Biophys. Acta 984 (1989) 214–224, https://doi.org/10.1016/0005-2736(89)90219-8.

[13] J.R. Henriksen, T.L. Andresen, L.N. Feldborg, L. Duelund, J.H. Ipsen, Understanding detergent effects on lipid membranes: a model study of lysolipids, Biophys. J. 98 (2010) 2199–2205, https://doi.org/10.1016/j.bpj.2010.01.037.

[14] A. Hildebrand, K. Beyer, R. Neubert, P. Garidel, A. Blume, Solubilization of negatively charged DPPC/DPPG liposomes by bile salts, J. Colloid Interface Sci. 279 (2004) 559–571, https://doi.org/10.1016/j.jcis.2004.06.085.

[15] J. Knol, K. Sjollema, B. Poolman, Detergent-mediated reconstitution of membrane proteins, Biochemistry 37 (1998) 16410–16415, https://doi.org/10.1021/bi981596u.

[16] L. Sun, J. Mao, Y. Zhao, C. Quan, M. Zhong, S. Fan, Coarse-grained molecular dynamics simulation of interactions between cyclic lipopeptide Bacillomycin D and cell membranes, Mol. Simul. 44 (2018) 346–376, https://doi.org/10.1080/08927022.2017.1384632.

[17] A. Pizzirusso, A. De Nicola, G.J. Sevink, A. Correa, M. Cascella, T. Kawakatsu, M. Rocco, Y. Zhao, M. Celino, G. Milano, Biomembrane solubilization mechanism by Triton X-100: a computational study of the three stage model, Phys. Chem. Chem. Phys. 19 (2017) 29780–29794, https://doi.org/10.1039/c7cp03871b.

[18] F. Szoka Jr., D. Papahadjopoulos, Comparative properties and methods of preparation of lipid vesicles (liposomes), Annu. Rev. Biophys. Bioeng. 9 (1980) 467–508, https://doi.org/10.1146/annurev.bb.09.060180.002343.

[19] G.E. Tiller, T.J. Mueller, M.E. Dockter, W.G. Struve, Hydrogenation of Triton X-100 eliminates its fluorescence and ultraviolet light absorption while preserving its detergent properties, Anal. Biochem. 141 (1984) 262–266, https://doi.org/10.1016/0003-2697(84)90455-X.

[20] K. Matsuzaki, O. Murase, K. Sugishita, S. Yoneyama, K. Akada, M. Ueha, A. Nakamura, S. Kobayashi, Optical characterization of liposomes by right angle light scattering and turbidity measurement, BBA – Biomembranes 1467 (2000) 219–226, https://doi.org/10.1016/S0005-2736(00)00223-6.

[21] R. Ashkar, M. Nagao, P.D. Butler, A.C. Woodka, M.K. Sen, T. Koga, Tuning membrane thickness fluctuations in model lipid bilayers, Biophys. J. 109 (2015) 106–112, https://doi.org/10.1016/j.bpj.2015.05.033.